

Cite this: *Chem. Sci.*, 2025, 16, 9337

All publication charges for this article have been paid for by the Royal Society of Chemistry

# Eliminating creep in vitrimers using temperature-resilient siloxane exchange chemistry and N-heterocyclic carbenes†

Tapas Debsharma,<sup>ab</sup> Loc Tan Nguyen,<sup>a</sup> Benon P. Maliszewski,<sup>c</sup> Susanne M. Fischer,<sup>a</sup> Vincent Scholiers,<sup>a</sup> Johan M. Winne,<sup>\*a</sup> Steven P. Nolan<sup>\*c</sup> and Filip E. Du Prez<sup>\*a</sup>

This study explores a novel N-heterocyclic carbene-mediated siloxane exchange mechanism, laying the foundation for designing covalent adaptable networks (CANs) with high temperature stability (>200 °C) for dynamic covalent chemistry. Small molecule siloxane compounds, obtained by hydrosilylation reactions, are used to demonstrate siloxane-exchange via a mechanism supported by density functional theory. The proposed mechanism presents an equilibrium, at elevated temperatures, between an imidazolium salt and its free carbene form, which is the catalytically active species. Following this mechanistic insight, a tetra-substituted ester-terminated siloxane cross-linker was synthesized and cured with a commercial amine hardener. The ensuing ester-amine reaction yields thermally stable, non-dynamic amide bonds, thereby enhancing material stability. The resulting CANs exhibit rapid stress relaxation at elevated temperatures and demonstrate successful recycling through compression molding without any significant loss of material properties. Remarkably, the synthesized material showcases high creep resistance, even up to 150 °C, indicating the benefits of having a thermally reversible catalyst system for siloxane activation. This ground-up design of dynamic chemistry and material synthesis not only presents innovative material design but also suggests avenues for exploring thermally stable, fast-exchanging and yet creep-resistant CANs.

Received 16th September 2024

Accepted 18th April 2025

DOI: 10.1039/d4sc06278g

rsc.li/chemical-science

## Introduction

Covalent adaptable networks (CANs) represent a relatively new class of cross-linked polymers that can undergo plastic deformation by exchanging covalent bonds upon external triggers, distinguishing them from traditional thermoset polymers.<sup>1</sup> Vitrimers are a type of CAN that undergoes an associative covalent bond exchange, that is, a bond-breaking event that is conditional upon a prior or simultaneous new bond-forming process, when exposed to heat.<sup>2</sup> Different chemistries have been explored to produce vitrimers, including transesterification,<sup>2,3</sup> boronic-ester chemistries,<sup>4,5</sup> transamination of vinylogous urethanes,<sup>6,7</sup> silicon-based chemistries,<sup>8,9</sup> thioether chemistry,<sup>10,11</sup> disulfide exchange<sup>12,13</sup> and others.<sup>14–19</sup>

However, many reported vitrimers face three main challenges: (1) the limited thermal stability (typically  $\leq 160$  °C) of the exchange chemistry, polymer matrix, or catalysts and sometimes combinations of these factors, reduce the scope of applications.<sup>5,6,10,15,20–23</sup> This is typically caused by polymer matrices such as polyimines, polyurethanes, and catalysts with limited thermal stability, that are metal-based, alkoxide-based or amine-based, which degrade upon exposure to air at elevated temperatures;<sup>24,25</sup> (2) the use of highly active catalysts raises concerns about the long-term stability of the produced materials in the environment<sup>11,16,26,27</sup> and (3) the susceptibility of vitrimers, and CANs in general, towards undesired deformations during the intended use—referred to as creep behavior—severely limits their industrial take-up.<sup>28–32</sup> Moreover, creep remains a common and challenging issue in fast-processable CANs.<sup>31</sup> The primary cause of creep in CANs is the bond exchange that occurs at elevated temperatures. Despite the steady expansion of the CAN library over the last decade, this novel type of polymer material is still vulnerable to creep deformations at service conditions. This limitation restricts their widespread adoption in practical applications such as in elastomers, composites, and adhesives.<sup>33</sup>

To address these limitations, various strategies have been deployed such as the incorporation of fillers, enhancement of

<sup>a</sup>Department of Organic and Macromolecular Chemistry, Ghent University, Krijgslaan 281-S4, 9000 Ghent, Belgium. E-mail: Filip.DuPrez@UGent.be; Johan.Winne@UGent.be

<sup>b</sup>Department of Chemistry, Indian Institute of Technology Kharagpur, 721302 Kharagpur, India

<sup>c</sup>Department of Chemistry and Centre for Sustainable Chemistry, Ghent University, Krijgslaan 281-S3, 9000 Ghent, Belgium. E-mail: Steven.Nolan@UGent.be

† Electronic supplementary information (ESI) available: NMR spectra, equation for calculation of swelling and soluble fraction, LC-MS spectrum, DSC thermograms, DMA data, stress-relaxation data, and amplitude sweep data are included. See DOI: <https://doi.org/10.1039/d4sc06278g>



crystallinity, phase separation, variation in cross-link density, quenching of exchangeable units, incorporations of static cross-links, catalyst control, concentration of exchangeable units, neighboring group participation effect, and utilization of supramolecular interactions.<sup>2,11,31,32,34–39</sup> In many cases, however, this improved dimensional stability invariably leads to deterioration of the (re)processability of CANs.<sup>40</sup> In the course of the past few years, silicon-based functionalities, for example, have been used to synthesize silicones for recycling and healing cracks by means of grinding and molding,<sup>41–46</sup> such as silyl ethers and siloxanes, that are well-known for their high-temperature stability, have attracted significant interest in the production of vitrimers and degradable materials.<sup>27,47–56</sup>

Compared to silyl ethers, siloxanes are more robust towards hydrolysis,<sup>9</sup> which is the reason why the siloxane functionality appears to be favored for vitrimer applications. Siloxane exchange is known to proceed *via* two different pathways. The first and most commonly used pathway, starting with pioneering works by Osthoff,<sup>57–59</sup> around the 1950s is a direct catalysis of siloxane exchange, by cleavage of Si–O–Si by a nucleophile, such as silanolates, cesium hydroxides, ammonium hydroxides,  $P_4^{-4}BuOH$ , *etc.* The nucleophile can also be a fluoride anion to activate siloxane exchange and is recently reported for siloxane-CANs that have been produced from several commodity plastics developed by Guan and coworkers (Fig. 1, left).<sup>9</sup> This strategy, however, resulted in high amounts of soluble fractions (up to ~50%) in the resulting materials. The second one—developed by some of us—employs the thermally (relatively) unstable 1,5,7-triazabicyclo [4.4.0]dec-5-ene catalyst (TBD), which is hypothesized to be a concerted pathway of siloxane exchange *via* activation of Si–O–Si cleavage and simultaneous addition of an alcoholic nucleophile. Montarnal and coworkers have given a deeper insight into the siloxane exchange mechanisms using different catalysts for silicone-based elastomers.<sup>53</sup>

The catalysts that are used for siloxane exchange typically promote effective siloxane exchange at elevated temperatures. That being said, most such catalysts have issues of thermal degradation with increasing temperature and typically struggle above 120 °C, with a few exceptions including fluoride catalysis as reported by Guan and coworkers.<sup>9</sup> On the other hand, the elevated temperature stability and high temperature creep

resistance of vitrimers is of utmost importance for a range of their application areas. In other words, the starting point of this study was the search for a thermally resilient catalyst to activate siloxane exchange.

Often, a compound that acts as a catalyst for the polymerization of monomers can simultaneously serve as a catalyst for functional group exchange in vitrimers. For example, TBD can be used for both polymerization of cyclic esters and mediates the transesterification reaction in vitrimers.<sup>60–62</sup> Similarly, TBD can polymerize cyclic siloxanes and also catalyze siloxane exchange.<sup>61,63</sup> Along the same line, we noticed that cyclic siloxanes can be polymerized by N-heterocyclic carbenes (NHCs).<sup>63</sup> NHCs can catalyze the cyclization reactions for the formation of

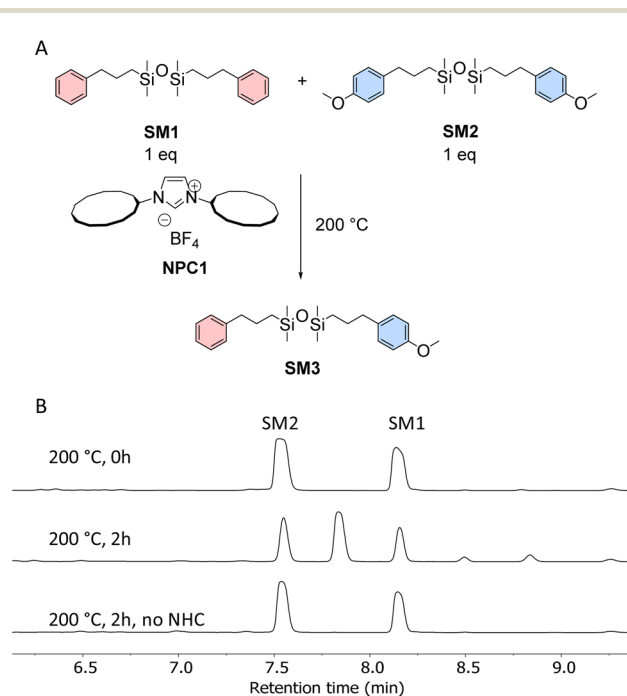


Fig. 2 (A) Chemical exchange between two siloxane molecules in the presence of NPC1 compound. (B) Liquid chromatography of the molecules SM1 and SM2, and for the chemical exchange study. The small signals between 8.5 and 9 minutes are attributed to impurities in the starting compounds.

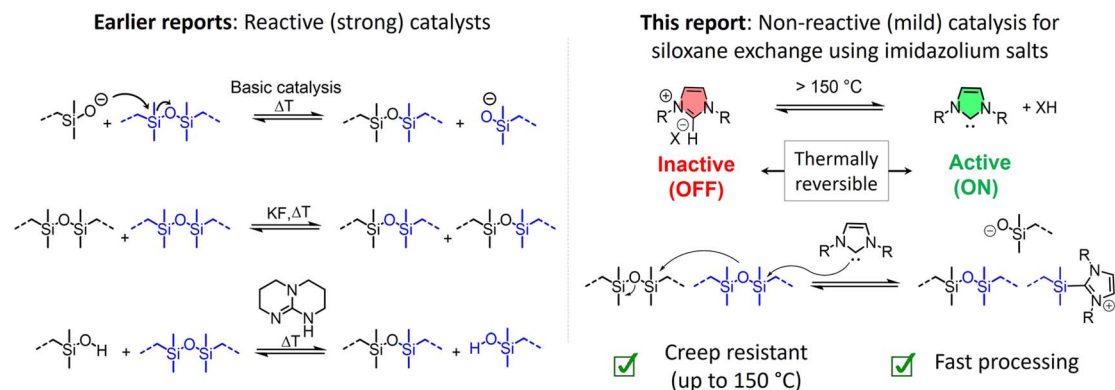


Fig. 1 Overview of previous approaches with reactive catalysts (left) and this research with non-reactive catalysts (right) for siloxane exchange in CANs.



$\beta$ -lactones, as well as transesterification reactions.<sup>64</sup> The cyclization and transesterification reactions are known to happen *via* nucleophilic addition of NHCs.<sup>64</sup> As NHCs are known to be generated *in situ* from imidazolium salts,<sup>65</sup> this inspired us to investigate N-heterocyclic carbene pre-catalysts (NPCs) for the siloxane exchange. Notably, several NPCs exhibit outstanding thermal stability ( $\geq 300$  °C, *e.g.* ionic liquids) and are frequently employed as solvents. In a vitrimer context, the ideal catalyst is the one that is (almost) inactive in promoting bond exchange at operational temperatures, which will also lead to significantly reduced creep deformation.<sup>31</sup>

In the present report, we showcase a novel pathway for activating siloxane exchange using temperature-resilient NPCs (Fig. 1, right). These NPCs are employed to demonstrate siloxane exchange through small molecule studies for which we propose a mechanistic pathway that is supported by density functional theory (DFT) calculations. Additionally, we report the synthesis of a siloxane containing ester terminated cross-linker that is cured with aliphatic amine hardeners. The resulting siloxane-containing vitrimers with NPCs are evaluated for key material properties such as thermal stability, degree of swelling, soluble fraction determination, reprocessing, stress relaxations, and creep behavior.

## Results and discussion

It is known that free carbenes and N-heterocyclic carbenes, in particular, can act as powerful nucleophilic catalysts for a range

of chemical reactions, including acyl transfer and silyl transfer reactions.<sup>66,67</sup>

Thus, we initially investigated a range of imidazolium salts as thermally stable ‘pre-catalysts’ that are expected to catalyze the silyl transfer between siloxanes. Imidazolium salts have been investigated as pre-catalyst, such as in polyester synthesis,<sup>68–70</sup> benzoin condensation,<sup>71</sup> and cyanosilylation.<sup>72</sup> Indeed, by loss of the relatively acidic C–H, a free carbene<sup>65,73</sup> or NHC can be reversibly generated, even though equilibrium concentrations of this neutral conjugate base can be expected to be very low at most temperatures, based on simple  $pK_a$ -considerations.<sup>74,75</sup> Typically, protected NHCs have been employed.<sup>65</sup> Such molecules, upon heating, release small molecules to generate NHCs *in situ*. The liberated small molecules can be alcoholic compounds, CO<sub>2</sub>, H<sub>2</sub>O, or metal complexes. In this study, we explored this thermo-reversible NHC formation for siloxane exchange in vitrimers.

At low and moderately elevated temperatures (<140 °C), siloxane exchange (between **SM1** and **SM2**, Fig. 2A) was indeed absent when imidazolium salts were added, which implies that the catalytic form of the NHC is not present under these conditions. However, we were very encouraged by the fact that significant siloxane exchange existed at higher temperatures (around 200 °C), without any obvious sign of degradation reactions for both the substrates and the pre-catalysts. We thus conducted a more in-depth investigation of these imidazolium salt-promoted silyl exchange equilibria, as a catalyst system with such a profile – no performance at low temperature, but

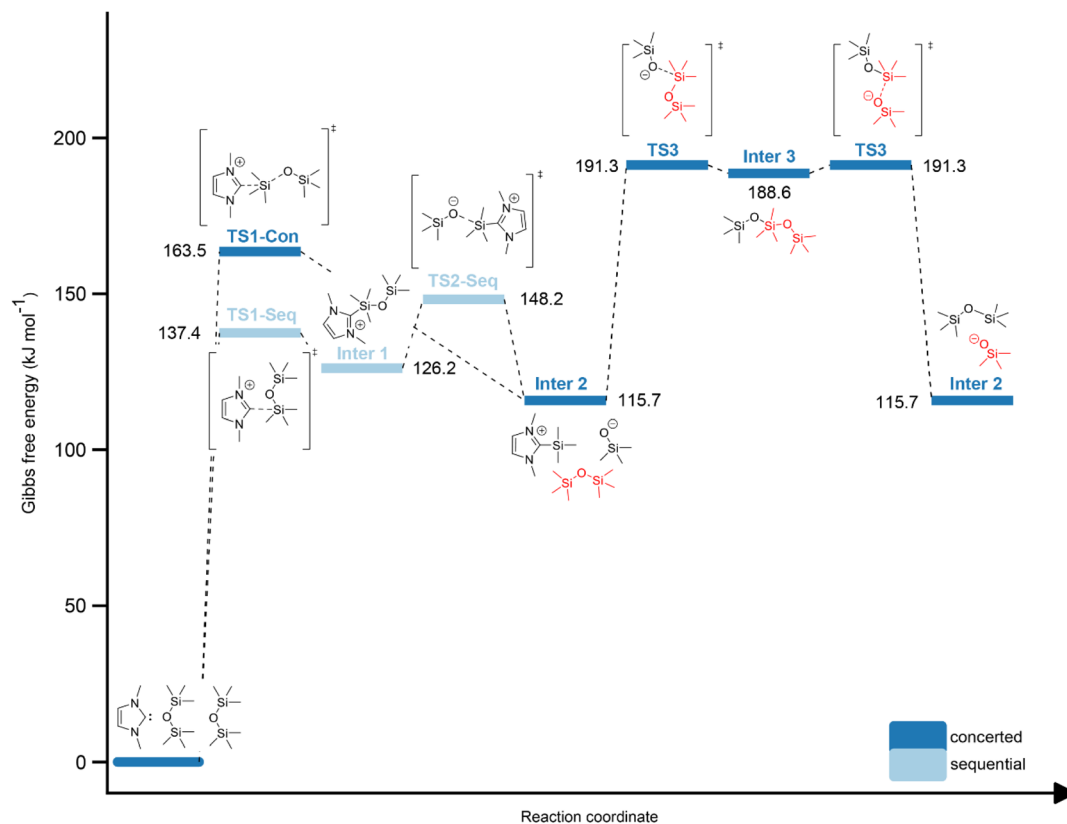


Fig. 3 Proposed pathway for siloxane exchange mediated by N-heterocyclic carbenes.



good performance at elevated temperatures—is very attractive for the design of CANs and vitrimers.<sup>76</sup>

To establish an NHC-catalyzed siloxane exchange through small molecule studies, two siloxane functionality-containing compounds (**SM1** and **SM2**) were prepared *via* hydrosilylation reactions<sup>77–79</sup> (ESI Section 3, Fig. S2–S7†). Subsequently, an imidazolium salt **NPC1** featuring bulky alkyl groups and a tetrafluoroborate ( $\text{BF}_4^-$ ) counter anion was synthesized (ESI Section 3, Fig. S8–S10†). The bulky alkyl substituted N-heterocyclic group was selected for better compatibility with the relatively apolar siloxane-based polymer matrix. The two siloxane compounds **SM1** and **SM2** were then heated together with **NPC1** at 200 °C in a septum-sealed vial for 2 h (Fig. 2A). In a separate vial, both compounds were also heated in the absence of any NHC precursors to serve as a control experiment. After 2 h, both samples were subjected to liquid chromatography mass spectrometry (LC-MS) analysis. While the reaction without imidazolium salt showed only two peaks, which are attributed to the two starting materials, the presence of the imidazolium salt in the other reaction vial led to the formation of a new peak, corresponding to a compound with a polarity between the two starting compounds (Fig. 2B). Despite its poor ionizability, the formation of exchange product **SM3** was observed by mass spectrometry (Fig. S11†). This observation suggests the exchange reaction between the two siloxane compounds in the presence of imidazolium salt. In addition, the  $^1\text{H}$  NMR analysis, which recorded no observable change, confirms the absence of significant side-product formation during the exchange reaction (Fig. S12†).

In classical N-heterocyclic carbene compound-catalyzed reactions, the presence of a Brønsted base is required to deprotonate the imidazolium salt, generating the corresponding free carbene.<sup>63,80</sup> While the typical  $\text{pK}_a$  value of imidazolium species ranges from 18 to 24 (in DMSO),<sup>74</sup> even weak bases like trimethylamine ( $\text{pK}_a$  9.0 in DMSO)<sup>81</sup> have demonstrated their effectiveness in generating the required amounts of active carbene species or adducts/complex to show catalytic activity. While a Brønsted base was not added to the reaction mixture in our experiments, we postulated the existence of an equilibrium between the imidazolium salt and a free carbene-containing entity at elevated temperatures ( $\geq 200$  °C).

The formation of a free carbene NHC is unavoidable given its well-known acid–base equilibria.<sup>75</sup>

In this context, it is relevant to note that Sardon and coworkers established a similar thermally promoted proton transfer for guanidinium salts, which have a very comparable  $\text{pK}_a$ -value.<sup>39</sup> Even though the concentration of free carbenes are low at all temperatures, as the equilibrium always favors the inert imidazolium salt, upon heating a switch will occur from catalytically irrelevant amounts of NHC to catalytically very relevant amounts.

On the other hand, the involvement of other low-abundant nucleophilic species, such as the anionic fluoride released from  $\text{BF}_4^-$ , should be considered. To further confirm the absence of such fluoride ion involvement from  $\text{BF}_4^-$  decomposition, two exchange experiments were conducted on **SM1** and **SM2** with the addition of: (a) fluoride-free NHC salt **NHC3**

(ESI Section 3, Fig. S13†); and (b) NHC-free fluoride salt  $\text{NaBF}_4$  under identical conditions. While **NHC3** catalyzed the exchange by showing an additional peak in the LC trace after 2 hours at 200 °C, no change was observed in the reaction including  $\text{NaBF}_4$  (Fig. S14†). In other words, those experiments further confirm the catalytic effect of NHC pieces and exclude the involvement of fluoride ion in the siloxane exchange.

Furthermore, to establish a plausible mechanism for the hypothesized exchange, density functional theory (DFT) calculations starting from the free carbene were carried out.

For this DFT-study, a sequential and a concerted pathway were investigated (Fig. 3). The sequential route starts with the addition of the imidazolium salt to the siloxane compound, resulting in the formation of a stable intermediate (**Inter1**) through a transition state (**TS1-Seq**) with an energy of  $137.4 \text{ kJ mol}^{-1}$ . This transition is mainly characterized by the rotation of the methyl groups and formation of the C–Si bond. Subsequently, **Inter1** collapses to form the respective silanolate species and imidazolium cation (**Inter2**). **TS2-Seq** exhibits an energy of  $148.2 \text{ kJ mol}^{-1}$ , implying that the silanolate anion is, expectedly, a poor leaving group. Notably, the relative difference in Gibbs free energy between **Inter2** and the starting compounds is merely  $115.7 \text{ kJ mol}^{-1}$ , rendering this transformation viable at temperatures around 200 °C. Alternatively, the concerted pathway for the initial step involves a backside attack of the NHC on the siloxane species in a nucleophilic

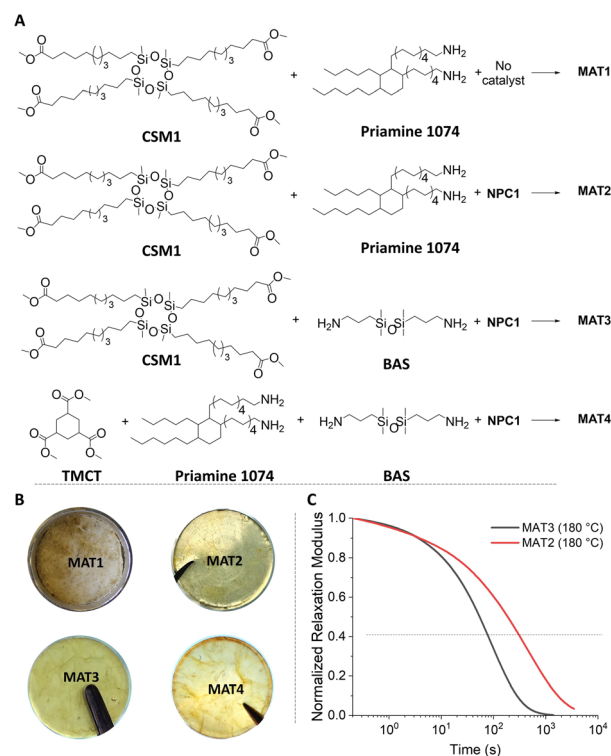


Fig. 4 (A) Scheme for the synthesis of siloxane containing materials with and without 10 mol% (with respect to siloxane) imidazolium catalyst. (B) Images of compression-molded samples from various material syntheses schematically presented in section-A (black objects on the images originate from tweezer-head). (C) Normalized stress-relaxation plots of MAT2 and MAT3 at 180 °C.



substitution reaction, leading directly to **Inter2**. The calculated reaction barrier for this reaction is  $163 \text{ kJ mol}^{-1}$ , which is slightly higher than that of the rate-determining step of the sequential mechanism. Once formed, the silanolate anion can engage in a concerted pathway with another siloxane molecule, thereby enabling the siloxane exchange. The calculated barrier for this subsequent reaction was determined to be  $75.6 \text{ kJ mol}^{-1}$  (energy difference between **Inter2** and **TS3**) and leads to a stable intermediate (**Inter 3**), which regenerates **Inter2** after collapsing. Thus, the potential energy surface (PES) exhibits triple-well characteristics featuring a pre- and post-TS before a central transition complex (**Inter 3**) for this reaction, which has been described previously for nucleophilic substitutions at Si atoms.<sup>82</sup>

In addition, an alternative mechanism was explored, starting from the imidazolium form of the catalyst. This approach was motivated by literature reports where the salt form of the carbene was identified to react with the substrate in a concerted manner without the need to generate the free carbene. However, a weak base was still present in these reactions.<sup>83–85</sup> In this case, the obtained activation barriers and energies of the intermediates are significantly higher compared to the free carbene pathways (ESI Section 5 and Fig. S1†).

It is worth emphasizing that carbene-silylium species, proposed as the exchange intermediate by DFT calculations, are known but are extremely unstable and thus challenging for their identification with NMR or LCMS analysis.<sup>86</sup> In an attempt to substantiate our mechanistic rationale, we conducted some studies to prepare these intermediates, but we could not isolate these transient species, indicating that they are highly reactive and short-lived species, as indicated by our DFT calculations (*vide supra*).

After the mechanistic rationalization of the NHC-catalyzed siloxane exchange, which points to a highly attractive and very temperature-responsive exchange profile, our subsequent endeavor involved the design of a polymer network. For this, we have chosen ester-terminated siloxane cross-linkers. This selection is motivated by the unique capability of amine-curing agents to react with ester groups during the cross-linking process. The ester-amine reaction results in the formation of thermally stable, non-dynamic amide bonds, contributing to the overall stability of the material and minimizing dynamic characteristics.<sup>87</sup> Moreover, the catalytic activity of the NHC can be expected to be enhanced in the resulting polymer network due to the possible presence of free amines as unreacted chain

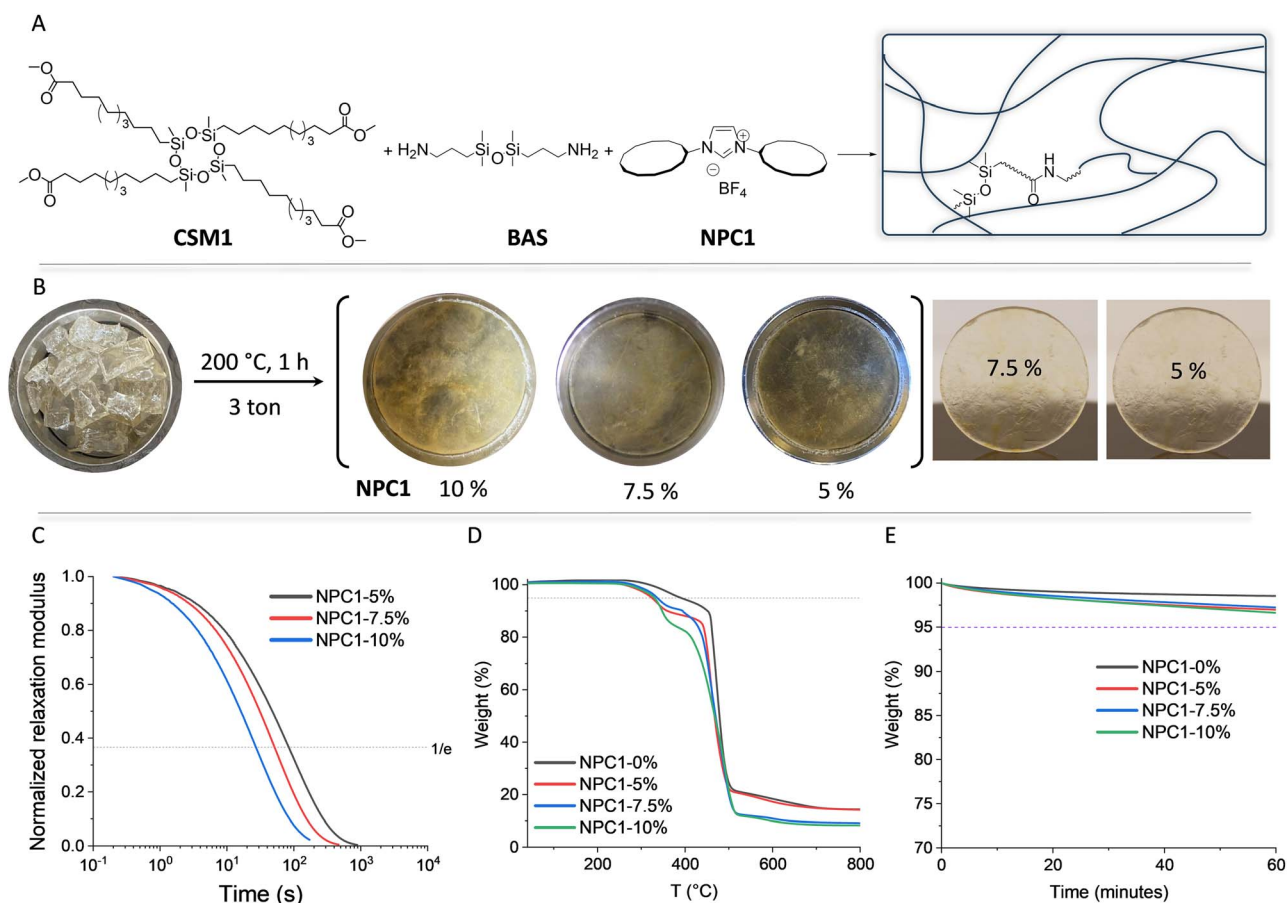


Fig. 5 (A) General scheme for the preparation of siloxane-containing polyamide polymer networks using different amounts of NPC1 catalyst. (B) Compression molding of different polymer networks containing various amounts of NPC1 catalyst. (C) Normalized stress relaxation of materials containing 5 mol%, 7.5 mol%, and 10 mol% (with respect to siloxane functionality) of NPC1 as catalysts at 250 °C. (D) TGA of samples containing varying amounts of NPC1 catalysts under N<sub>2</sub>. (E) Isothermal TGA at 250 °C of samples containing varying amounts of NPC1 catalysts under N<sub>2</sub>.



ends, and as weak bases to promote imidazolium salt deprotonation.

To produce reprocessable siloxane-containing polymer networks, a few monomers were selected such as the ester-terminated siloxane cross-linker compound **CSM1** (2,4,6,8-tetramethyl-1,3,5,7,2,4,6,8-tetraoxatetrasiloxane-2,4,6,8-tetrayl) tetraundecanoate), **TMCT** (trimethyl cyclohexane-1,3,5-tricarboxylate), **Priamine 1074**, and **BAS 1,3-bis(3-aminopropyl)tetramethyldisiloxane**). **CSM1** was synthesized from commercially available cyclic siloxane 2,4,6,8-tetramethylcyclotetrasiloxane through a simple single-step hydro-silylation reaction. The resulting compound was purified by distillation and characterized by  $^1\text{H}$ ,  $^{13}\text{C}$ , and HSQC NMR spectroscopy (ESI Section 3, Fig. S15–S17 $^\dagger$ ). **TMCT** was synthesized *via* esterification of cyclohexane-1,3,5-tricarboxylic acid (ESI Section 3, and Fig. S18 and S19 $^\dagger$ ).

We prepared siloxane-containing materials with and without **NPC1** (*i.e.*, 10 or 0 mol% with respect to siloxane functionality) catalyst, namely **MAT1**, **MAT2**, **MAT3**, and **MAT4** (Fig. 4A). The samples were then compression-molded at 200 °C under 3 tons of pressure for 1 h. **MAT1** showed no healing ability under the deployed condition because of the absence of any siloxane exchange catalyst. On the other hand, **MAT2**, **MAT3**, and **MAT4** could be compression-molded to smooth discs (Fig. 4B), suggesting that the siloxane exchange is catalyzed by the **NPC1** catalyst. **MAT4** turned out to be too brittle to prepare samples for rheology. This brittleness can be attributed to the high cross-link density because of the reaction between small molecules **TMCT** and **BAS**. This composition was therefore not considered for further characterization.

**MAT3** turned out to be faster in terms of stress relaxation than **MAT2** (Fig. 4C). This is ascribed to the short amine

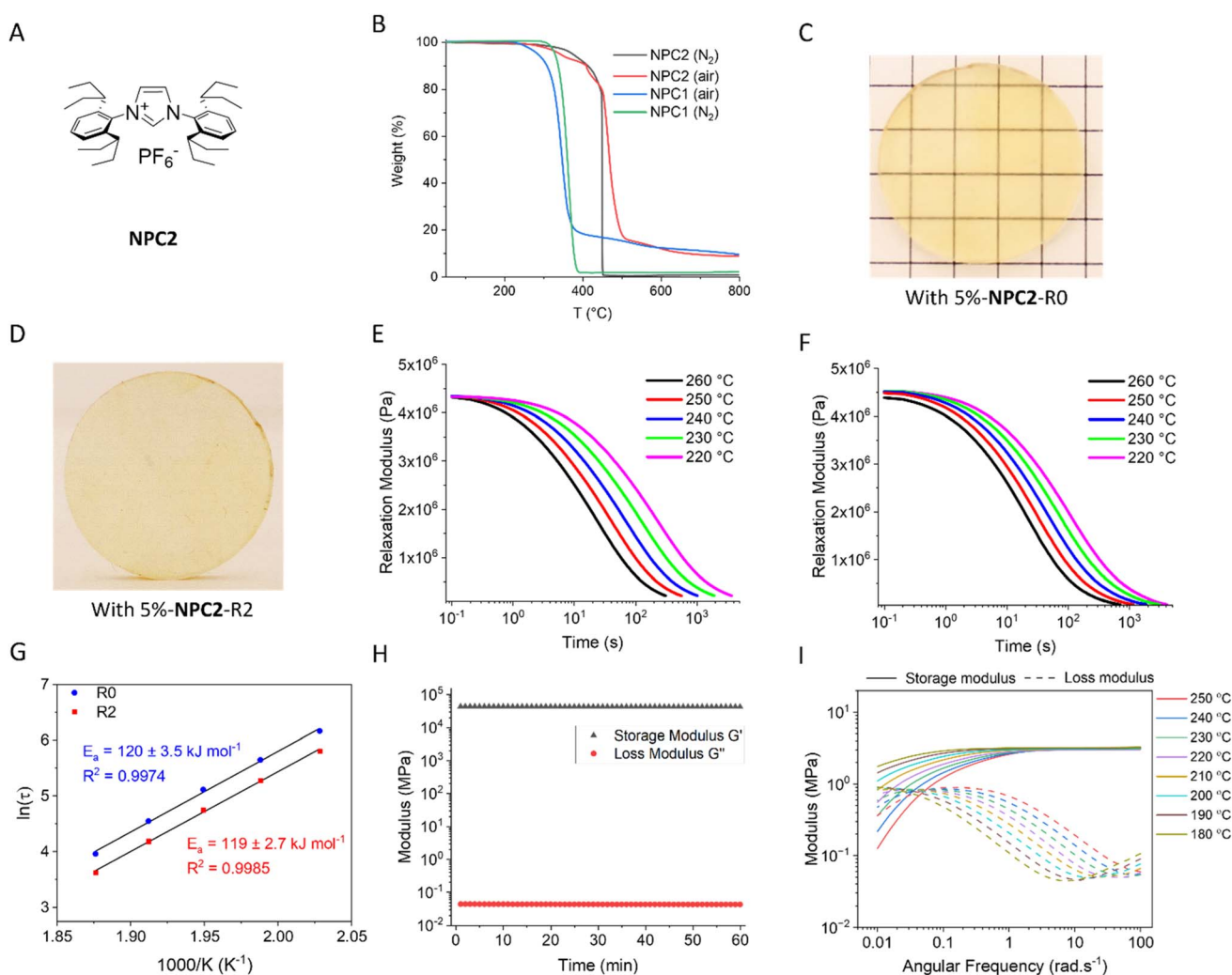


**Fig. 6** (A) Chemical structure of the NPC2 catalyst (B) TGA analysis of NPC1 and NPC2 in air and nitrogen environment. (C) R0: First compression molded siloxane-containing polyamide networks with 5%-NPC2. (D) R2: Third compression molded siloxane-containing polyamide networks with 5%-NPC2. (E) Non-normalized stress-relaxation data for 5%-NPC2 containing R0 samples recycled *via* compression molding at various temperatures ranging from 220 °C to 260 °C with 10 °C intervals. (F) Non-normalized stress-relaxation data for 5%-NPC2 containing R2 samples recycled *via* compression molding at various temperatures ranging from 220 °C to 260 °C with 10 °C intervals. (G) Arrhenius activation energies of stress relaxation for the materials recycled materials containing 5%-NPC2 catalysts. (H) Time sweep data for R0 sample with 5%-NPC2 at 200 °C with 1% of shear strain and fixed frequency of 1 Hz. (I) Frequency sweep data of R0 sample with 5%-NPC2.



hardener BAS (in the case of **MAT3**), which facilitates the closer proximity of exchangeable siloxane functional groups compared to the much longer Priamine 1074 in **MAT2**. Moreover, BAS contains an additional siloxane group which is absent in Priamine 1074. With these results in hand, we proceeded with the material composition of **MAT3** in combination with a suitable siloxane exchange activating NPC.

The ester-terminated siloxane cross-linker, **CSM1**, was reacted with BAS to prepare a set of materials with varying amounts of **NPC1**: 0 mol%, 5 mol%, 7.5 mol%, and 10 mol%. Samples containing 5 or higher mol% of **NPC1** could be compression-molded to a smooth disc (Fig. 5A and B). For the samples with varying amounts of **NPC1**, the stress-relaxation is understandably faster with higher NPC content as revealed by stress relaxation experiments at 250 °C (Fig. 5C), which is well below the 1% weight loss temperature ( $T_{d1\%} > 280$  °C for all the samples as shown in Fig. 5D and E). Furthermore, the samples having higher imidazolium salt content also appeared opaquer (Fig. 5B). While the sample with only 5 %-**NPC1** content showed sufficiently fast stress relaxation ( $\tau^* = 84$  s), it still exhibited some level of opaqueness and was visibly phase separating (Fig. 5B), suggesting compatibility issues between the imidazolium salt compound and the polymer matrix. To address this, **NPC1** compound was replaced with **NPC2** (Fig. 6A, ESI Section 3, and Fig. S20–S22†) for material synthesis. The choice of **NPC2**, containing bulky aryl groups, was made to achieve better compatibility with the apolar polymer matrix, while the hexafluorophosphate ( $\text{PF}_6^-$ ) counter anion was selected because ionic liquids containing this  $\text{PF}_6^-$  anion are known to be among the most thermally stable NPCs.<sup>88</sup> Indeed, as observed in TGA, **NPC2** exhibited greater thermal stability than **NPC1** (Fig. 6B). Gratifyingly, the material containing 5% **NPC2** was fully transparent (Fig. 6C and D). Therefore, samples prepared with 5 %-**NPC2**, showing a glass transition temperature ( $T_g$ ) of ca. 2 °C (Fig. S23†), were used for further analysis.

To demonstrate the recyclability of these materials, pristine samples containing 5 %-**NPC2** were cut into small pieces and compression-molded into a smooth disc at 200 °C, at which no significant degradation was observed by TGA and a time sweep experiment (Fig. S24†). This recycling process was repeated for two additional cycles, denoted as R0, R1, and R2, where R0 represents the sample that underwent the first recycling cycle by compression molding. Stress relaxation experiments between 220 and 260 °C on R0 and R2 revealed consistent stress relaxation times with an activation energy of about 139 kJ mol<sup>-1</sup> (Fig. 6E–G), fitted by the stretched Maxwell model (Fig. S25, and Table S2†).

Additionally, the degree of swelling and soluble fractions remained nearly the same over different recycling steps (Table S1†). Finally, the FTIR analysis (Fig. S26†) of both R0 and R2 samples shows no significant change in chemical composition.

This analysis confirms the high-temperature resilient dynamic nature of the materials during reprocessing.

It is important to note that the non-normalized stress relaxation modulus at early relaxation times remained practically constant (Fig. 6E and F) for different temperatures, suggesting an associative character of the exchange chemistry as

was also suggested by the proposed mechanism discussed above.

This associative nature is further supported by a constant storage modulus in both time (Fig. 6H) and frequency sweep experiments at varying temperatures (Fig. 6I), which shows a constant storage and loss modulus over 60 min.

Having established a novel siloxane exchange pathway, catalyzed by N-heterocyclic carbenes, and having successfully demonstrated the recyclability of the corresponding vitrimers, we aimed to investigate the creep resistance of these materials, which is frequently absent in CAN materials. To assess the creep deformation behavior of the materials containing 5% **NPC2**, creep-no-recovery experiments were conducted over a wide temperature interval (60–150 °C). For this purpose, a shear stress of 2000 Pa was applied, and the resulting strain was recorded over time. Power law scaling of the derived creep compliance  $J(t)$  is expected to be unity when a material reaches terminal relaxation.<sup>89</sup> This power law scaling is crucial for accurately estimating the unique zero-shear viscosity  $\eta_0$  and creep rate  $\dot{\epsilon}$  at a given temperature.<sup>90</sup> However, the material containing 5%-**NPC2** did not exhibit this steady-state behavior. Instead, only a power law scaling of 0.16 was observed after 15 000 s of measurement time at 150 °C (Fig. 7).

In other words, this implies that the material's response is dominated by instantaneous deformations and primary creep effects but did not achieve terminal relaxation (viscous behavior), making it not feasible to derive meaningful estimations for  $\eta_0$  or  $\dot{\epsilon}$ . Nonetheless, it is noteworthy that virtually no (primary) creep could be observed, even up to temperatures as

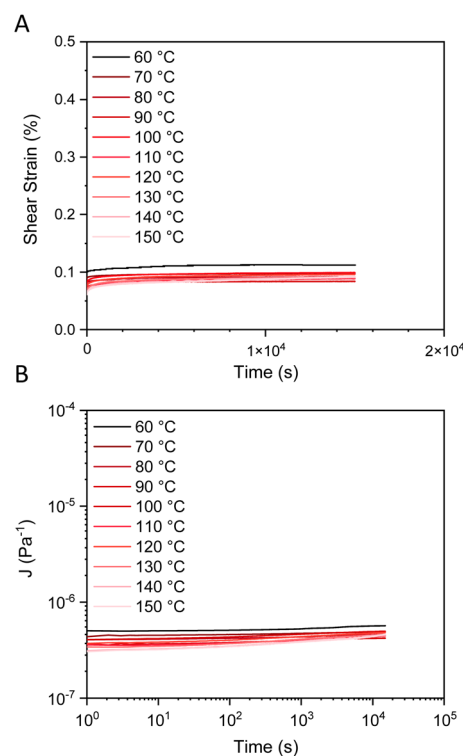


Fig. 7 Strain vs. time (A) and creep compliance with time (B) plots for the R0 materials containing 5%-**NPC2**.



high as 150 °C, showcasing an unprecedented creep resistance in elastomeric dynamic materials. The same experiment conducted on R2 materials yielded consistent results within experimental error (Fig. S27†). Such high creep resistance of the vitrimers, including in the recycled samples, is ascribed to the siloxane exchange catalyzed by thermally reversible NHC pre-catalysts.

## Conclusions

Herein, we introduce a novel siloxane exchange catalyzed by 'dormant' N-heterocyclic carbenes (NHCs), which can be added to polymer formulations as relatively inert imidazolium salts. This siloxane exchange mechanism, with an endothermic proton exchange that releases reactive free carbenes at high temperatures to engage siloxanes as a nucleophilic catalyst, is established through small molecule studies and density functional theory (DFT) calculations. The NHC-imidazolium equilibrium results in an attractive thermally reversible catalyst system that is inactive at low to medium temperatures (up to 150 °C), while it is highly active at higher temperatures.

Together with the excellent thermal stabilities of the moieties involved in the polymer networks (*i.e.*, amides, siloxanes, and imidazolium salts), this results in a highly attractive design principle for vitrimers, while being limited for some other polymer matrices by the reactive nature of carbenes. The networks showed a clear dependence on catalyst loading. The obtained siloxane-containing polyamide networks exhibit remarkable thermal stability ( $T_{d1\%} > 275$  °C) and high gel fractions. The materials including the catalyst were further reprocessed *via* compression molding without significantly deteriorating the stress relaxation time and other material properties such as swelling degrees, soluble fractions, and glass transition temperatures. Notably, despite demonstrating rapid stress-relaxation at 250 °C, the materials showed significant creep resistance, even at elevated temperatures up to 150 °C.

Thus, the presented strategy reconciles rapid stress dissipation with creep resistance, which is highly sought after in the design of vitrimer materials and CANs. Finally, the study shows that catalytic systems that have been developed for performance in classical chemical reactions are usually not ideally suited for the activation of vitrimers. Indeed, the temperature responsiveness of a catalyst (dormant at low temperature and only active at high temperatures) is normally a non-desirable feature of a catalyst. As a broader perspective, this work shows that vitrimer design can benefit from exploring non-classical (more inert) additives as a catalyst, or that catalyst design needs to be considered in an alternative way in such sustainable material design.

## Author contributions

This manuscript was written through contributions of all authors. All authors have given approval to the final version of the manuscript.

## Conflicts of interest

The authors declare no conflict of interest.

## Data availability

The data supporting this article have been included as part of the Supplementary Information.†

## Acknowledgements

This project has received funding from the European Research Council (ERC) under the European Union's Horizon 2020 research and innovation programme 101021081 (ERC-AdG-2020, CiMaC-project) and from the iBOF-project C3 (01IB1020). The authors thank Bernhard De Meyer and Jan Goeman for their technical assistance and Dr Nezha Badi for fruitful discussions. V. S. would like to thank the Research Foundation Flanders (FWO) (Application 1S34725N) for financial support. The resources and services used for DFT calculation in this work were provided by the VSC (Flemish Supercomputer Center), funded by the Research Foundation – Flanders (FWO) and the Flemish Government. The FWO is acknowledged for a PhD fellowship to B. P. M. (1SB5321N). Umicore AG and Johnson Matthey are thanked for generous gifts of materials. The NMR expertise centre (Ghent University) is also acknowledged for providing support and access to NMR infrastructure funded by a Research Foundation Flanders (FWO I006920N & Hercules foundation AUGE/09/2006) and the Bijzonder Onderzoeksfonds (BOF.BAS.2022.0023.01).

## Notes and references

- C. J. Kloxin, T. F. Scott, B. J. Adzima and C. N. Bowman, Covalent Adaptable Networks (CANs): A Unique Paradigm in Cross-Linked Polymers, *Macromolecules*, 2010, **43**, 2643–2653.
- D. Montarnal, M. Capelot, F. Tournilhac and L. Leibler, Silica-Like Malleable Materials from Permanent Organic Networks, *Science*, 2011, **334**, 965–968.
- M. Delahaye, J. M. Winne and F. E. Du Prez, Internal Catalysis in Covalent Adaptable Networks: Phthalate Monoester Transesterification As a Versatile Dynamic Cross-Linking Chemistry, *J. Am. Chem. Soc.*, 2019, **141**, 15277–15287.
- M. Röttger, T. Domenech, R. van der Weegen, A. Breuillac, R. Nicolaÿ and L. Leibler, High-performance vitrimers from commodity thermoplastics through dioxaborolane metathesis, *Science*, 2017, **356**, 62–65.
- Y. Zhao, T. Qin, C. Jiang, J. Li, Y. Xiong, S. Liu, J. Qin, X. Shi and G. Zhang, Boronic ester-based vitrimeric methylvinyl silicone elastomer with "solid-liquid" feature and rate-dependent mechanical performance, *Polymer*, 2023, **265**, 125545.
- W. Denissen, G. Rivero, R. Nicolaÿ, L. Leibler, J. M. Winne and F. E. Du Prez, Vinylogous Urethane Vitrimers, *Adv. Funct. Mater.*, 2015, **25**, 2451–2457.



- 7 W. Denissen, M. Droesbeke, R. Nicolaÿ, L. Leibler, J. M. Winne and F. E. Du Prez, Chemical control of the viscoelastic properties of vinylogous urethane vitrimers, *Nat. Commun.*, 2017, **8**, 14857.
- 8 C. A. Tretbar, J. A. Neal and Z. Guan, Direct Silyl Ether Metathesis for Vitrimers with Exceptional Thermal Stability, *J. Am. Chem. Soc.*, 2019, **141**, 16595–16599.
- 9 C. Tretbar, J. Castro, K. Yokoyama and Z. Guan, Fluoride-Catalyzed Siloxane Exchange as a Robust Dynamic Chemistry for High-Performance Vitrimers, *Adv. Mater.*, 2023, **35**, 2303280.
- 10 B. Hendriks, J. Waelkens, J. M. Winne and F. E. Du Prez, Poly(thioether) Vitrimers via Transalkylation of Trialkylsulfonium Salts, *ACS Macro Lett.*, 2017, **6**, 930–934.
- 11 V. Scholiers, B. Hendriks, S. Maes, T. Debsharma, J. M. Winne and F. E. Du Prez, Trialkylsulfonium-Based Reprocessable Polyurethane Thermosets, *Macromolecules*, 2023, **56**, 9559–9569.
- 12 G. Kim, C. Caglayan and G. J. Yun, Epoxy-Based Catalyst-Free Self-Healing Elastomers at Room Temperature Employing Aromatic Disulfide and Hydrogen Bonds, *ACS Omega*, 2022, **7**, 44750–44761.
- 13 A. Roig, M. Agizza, À. Serra and S. De la Flor, Disulfide vitrimeric materials based on cystamine and diepoxy eugenol as bio-based monomers, *Eur. Polym. J.*, 2023, **194**, 112185.
- 14 R. L. Snyder, D. J. Fortman, G. X. De Hoe, M. A. Hillmyer and W. R. Dichtel, Reprocessable Acid-Degradable Polycarbonate Vitrimers, *Macromolecules*, 2018, **51**, 389–397.
- 15 A. J. Melchor Bañales and M. B. Larsen, Thermal Guanidine Metathesis for Covalent Adaptable Networks, *ACS Macro Lett.*, 2020, **9**, 937–943.
- 16 Y.-X. Lu and Z. Guan, Olefin Metathesis for Effective Polymer Healing via Dynamic Exchange of Strong Carbon–Carbon Double Bonds, *J. Am. Chem. Soc.*, 2012, **134**, 14226–14231.
- 17 M. Guerre, C. Taplan, J. M. Winne and F. E. Du Prez, Vitrimers: directing chemical reactivity to control material properties, *Chem. Sci.*, 2020, **11**, 4855–4870.
- 18 Y. Tao, X. Liang, J. Zhang, I. M. Lei and J. Liu, Polyurethane vitrimers: chemistry, properties and applications, *J. Polym. Sci.*, 2023, **61**, 2233–2253.
- 19 H. Memon, Y. Wei, L. Zhang, Q. Jiang and W. Liu, An imine-containing epoxy vitrimer with versatile recyclability and its application in fully recyclable carbon fiber reinforced composites, *Compos. Sci. Technol.*, 2020, **199**, 108314.
- 20 S. Dhers, G. Vantomme and L. Avérous, A fully bio-based polyimine vitrimer derived from fructose, *Green Chem.*, 2019, **21**, 1596–1601.
- 21 R. Hajj, A. Duval, S. Dhers and L. Avérous, Network Design to Control Polyimine Vitrimer Properties: Physical Versus Chemical Approach, *Macromolecules*, 2020, **53**, 3796–3805.
- 22 K. Liang, G. Zhang, J. Zhao, L. Shi, J. Cheng and J. Zhang, Malleable, Recyclable, and Robust Poly(amide-imine) Vitrimers Prepared through a Green Polymerization Process, *ACS Sustain. Chem. Eng.*, 2021, **9**, 5673–5683.
- 23 A. Zych, J. Tellers, L. Bertolacci, L. Ceseracciu, L. Marini, G. Mancini and A. Athanassiou, Biobased, Biodegradable, Self-Healing Boronic Ester Vitrimers from Epoxidized Soybean Oil Acrylate, *ACS Appl. Polym. Mater.*, 2021, **3**, 1135–1144.
- 24 A. K. Voice, F. Closmann and G. T. Rochelle, Oxidative Degradation of Amines With High-Temperature Cycling, *Energy Procedia*, 2013, **37**, 2118–2132.
- 25 T. Arii and A. Kishi, The effect of humidity on thermal process of zinc acetate, *Thermochim. Acta*, 2003, **400**, 175–185.
- 26 P. Zheng and T. J. McCarthy, A Surprise from 1954: Siloxane Equilibration Is a Simple, Robust, and Obvious Polymer Self-Healing Mechanism, *J. Am. Chem. Soc.*, 2012, **134**, 2024–2027.
- 27 X. Wu, X. Yang, R. Yu, X.-J. Zhao, Y. Zhang and W. Huang, A facile access to stiff epoxy vitrimers with excellent mechanical properties via siloxane equilibration, *J. Mater. Chem. A*, 2018, **6**, 10184–10188.
- 28 A. M. Hubbard, Y. Ren, C. R. Picu, A. Sarvestani, D. Konkolewicz, A. K. Roy, V. Varshney and D. Nepal, Creep Mechanics of Epoxy Vitrimer Materials, *ACS Appl. Polym. Mater.*, 2022, **4**, 4254–4263.
- 29 Y. Liu, Z. Tang, D. Wang, S. Wu and B. Guo, Biomimetic design of elastomeric vitrimers with unparalleled mechanical properties, improved creep resistance and retained malleability by metal–ligand coordination, *J. Mater. Chem.*, 2019, **7**, 26867–26876.
- 30 W. Liu, D. F. Schmidt and E. Reynaud, Catalyst Selection, Creep, and Stress Relaxation in High-Performance Epoxy Vitrimers, *Ind. Eng. Chem.*, 2017, **56**, 2667–2672.
- 31 F. Van Lijsebetten, T. Debsharma, J. M. Winne and F. E. Du Prez, A Highly Dynamic Covalent Polymer Network without Creep: Mission Impossible?, *Angew. Chem., Int. Ed.*, 2022, **61**, e202210405.
- 32 F. Van Lijsebetten, K. De Bruycker, Y. Spiesschaert, J. M. Winne and F. E. Du Prez, Suppressing Creep and Promoting Fast Reprocessing of Vitrimers with Reversibly Trapped Amines, *Angew. Chem., Int. Ed.*, 2022, **61**, e202113872.
- 33 B. Slay and W. Webber, *Stress relaxation of elastomer compounds*, Sealing Technology, 2011, 2011, pp. 9–12.
- 34 T. Stukenbroeker, W. Wang, J. M. Winne, F. E. Du Prez, R. Nicolaÿ and L. Leibler, Polydimethylsiloxane quenchable vitrimers, *Polym. Chem.*, 2017, **8**, 6590–6593.
- 35 L. Li, X. Chen, K. Jin and J. M. Torkelson, Vitrimers Designed Both To Strongly Suppress Creep and To Recover Original Cross-Link Density after Reprocessing: Quantitative Theory and Experiments, *Macromolecules*, 2018, **51**, 5537–5546.
- 36 J. J. Cash, T. Kubo, D. J. Dobbins and B. S. Sumerlin, Maximizing the symbiosis of static and dynamic bonds in self-healing boronic ester networks, *Polym. Chem.*, 2018, **9**, 2011–2020.
- 37 C. Dertnig, G. Guedes de la Cruz, D. Neshchadin, S. Schlögl and T. Griesser, Blocked Phosphates as Photolabile Catalysts for Dynamic Photopolymer Networks, *Angew. Chem., Int. Ed.*, 2023, **62**, e202215525.
- 38 D. Reisinger, M. U. Kriehuber, M. Bender, D. Bautista-Anguis, B. Rieger and S. Schlögl, Thermally Latent Bases in



- Dynamic Covalent Polymer Networks and their Emerging Applications, *Adv. Mater.*, 2023, **35**, 2300830.
- 39 G. Vozzolo, M. Ximenis, D. Mantione, M. Fernández and H. Sardon, Thermally Reversible Organocatalyst for the Accelerated Reprocessing of Dynamic Networks with Creep Resistance, *ACS Macro Lett.*, 2023, **12**, 1536–1542.
- 40 G. J. M. Formon, S. Storch, A. Y.-G. Delplanque, B. Bresson, N. J. Van Zee and R. Nicolaÿ, Overcoming the Tradeoff Between Processability and Mechanical Performance of Elastomeric Vitrimers, *Adv. Funct. Mater.*, 2023, **33**, 2306065.
- 41 B. Rupasinghe and J. C. Furgal, Full Circle Recycling of Polysiloxanes *via* Room-Temperature Fluoride-Catalyzed Depolymerization to Repolymerizable Cyclics, *ACS Appl. Polym. Mater.*, 2021, **3**, 1828–1839.
- 42 M. Weidauer, B. Heyder, D. Woelki, M. Tschiersch, A. Köhler-Krützfeldt and S. Enthaler, Iron-catalyzed depolymerizations of end-of-life silicones with fatty alcohols, *Resour.-Effic. Technol.*, 2015, **1**, 73–79.
- 43 S. Enthaler, Zinc-Catalyzed Depolymerization of End-of-Life Polysiloxanes, *Angew. Chem., Int. Ed.*, 2014, **53**, 2716–2721.
- 44 D. J. Krug, M. Z. Asuncion and R. M. Laine, Facile Approach to Recycling Highly Cross-Linked Thermoset Silicone Resins under Ambient Conditions, *ACS Omega*, 2019, **4**, 3782–3789.
- 45 C.-L. Chang, H. S.-J. Lee and C.-K. Chen, Nucleophilic Cleavage of Crosslinked Polysiloxanes to Cyclic Siloxane Monomers: Mild Catalysis by a Designed Polar Solvent System, *J. Polym. Res.*, 2005, **12**, 433–438.
- 46 M. R. Alexander, F. S. Mair, R. G. Pritchard and J. E. Warren, Mild depolymerization of silicone grease using aluminum(III)chloride: high-yield synthesis and crystal structure of  $[\{ClSiMe_2OAlCl_2\}_2]$ , and its controlled hydrolysis on aluminum surfaces, *Appl. Organometal. Chem.*, 2003, **17**, 730–734.
- 47 H. Fouilloux, M.-N. Rager, P. Ríos, S. Conejero and C. M. Thomas, Highly Efficient Synthesis of Poly(silylether)s: Access to Degradable Polymers from Renewable Resources, *Angew. Chem., Int. Ed.*, 2022, **61**, e202113443.
- 48 C. Cheng, A. Watts, M. A. Hillmyer and J. F. Hartwig, Polysilylether: A Degradable Polymer from Biorenewable Feedstocks, *Angew. Chem., Int. Ed.*, 2016, **55**, 11872–11876.
- 49 K. E. L. Husted, C. M. Brown, P. Shieh, I. Kevlishvili, S. L. Kristufek, H. Zafar, J. V. Accardo, J. C. Cooper, R. S. Klausen, H. J. Kulik, J. S. Moore, N. R. Sottos, J. A. Kalow and J. A. Johnson, Remolding and Deconstruction of Industrial Thermosets *via* Carboxylic Acid-Catalyzed Bifunctional Silyl Ether Exchange, *J. Am. Chem. Soc.*, 2023, **145**, 1916–1923.
- 50 M. O. Saed and E. M. Terentjev, Catalytic Control of Plastic Flow in Siloxane-Based Liquid Crystalline Elastomer Networks, *ACS Macro Lett.*, 2020, **9**, 749–755.
- 51 M. O. Saed and E. M. Terentjev, Siloxane crosslinks with dynamic bond exchange enable shape programming in liquid-crystalline elastomers, *Sci. Rep.*, 2020, **10**, 6609.
- 52 M. S. Islam, G. Kedziora, J. Lee, A. Stafford, V. Varshney, D. Nepal, L. A. Baldwin and A. K. Roy, Efficiency and Mechanism of Catalytic Siloxane Exchange in Vitri-mer Polymers: Modeling and Density Functional Theory Investigations, *J. Phys. Chem. A*, 2024, **128**, 5627–5636.
- 53 D. Z. Khedaoui, C. Tribout, J. Bratananu, F. D'Agosto, C. Boisson and D. Montarnal, Deciphering Siloxane Bond Exchanges: From a Molecular Study to Vitri-merization and Recycling of Silicone Elastomers, *Angew. Chem., Int. Ed.*, 2023, **62**, e202300225.
- 54 B. Yi, S. Wang, C. Hou, X. Huang, J. Cui and X. Yao, Dynamic siloxane materials: From molecular engineering to emerging applications, *Chem. Eng. J.*, 2021, **405**, 127023.
- 55 A. A. Putnam-Neeb, A. Stafford, S. Babu, S. J. Chapman, C. M. Hemmingsen, M. S. Islam, A. K. Roy, J. A. Kalow, V. Varshney, D. Nepal and L. A. Baldwin, Oligosiloxane-Based Epoxy Vitrimers: Adaptable Thermosetting Networks with Dual Dynamic Bonds, *ACS Appl. Polym. Mater.*, 2024, **6**(23), 14229–14234.
- 56 S. Fadlallah, F. Van Lijsebetten, T. Debsharma, V. Scholiers, F. Allais and F. E. Du Prez, Exploring the dual dynamic synergy of transesterification and siloxane exchange in vitrimers, *Eur. Polym. J.*, 2024, **213**, 113117.
- 57 D. T. Hurd, R. C. Osthoff and M. L. Corrin, The Mechanism of the Base-catalyzed Rearrangement of Organopolysiloxanes<sup>1</sup>, *J. Am. Chem. Soc.*, 1954, **76**, 249–252.
- 58 S. W. Kantor, W. T. Grubb and R. C. Osthoff, The Mechanism of the Acid- and Base-catalyzed Equilibration of Siloxanes, *J. Am. Chem. Soc.*, 1954, **76**, 5190–5197.
- 59 R. C. Osthoff, A. M. Bueche and W. T. Grubb, Chemical Stress-Relaxation of Polydimethylsiloxane Elastomers<sup>1</sup>, *J. Am. Chem. Soc.*, 1954, **76**, 4659–4663.
- 60 L. Simón and J. M. Goodman, The Mechanism of TBD-Catalyzed Ring-Opening Polymerization of Cyclic Esters, *J. Org. Chem.*, 2007, **72**, 9656–9662.
- 61 T. Debsharma, V. Amfilochiou, A. A. Wróblewska, I. De Baere, W. Van Paeppegem and F. E. Du Prez, Fast Dynamic Siloxane Exchange Mechanism for Reshapable Vitri-mer Composites, *J. Am. Chem. Soc.*, 2022, **144**, 12280–12289.
- 62 T. Debsharma, S. Engelen, I. De Baere, W. Van Paeppegem and F. Du Prez, Resorcinol-Derived Vitrimers and Their Flax Fiber-Reinforced Composites Based on Fast Siloxane Exchange, *Macromol. Rapid Commun.*, 2023, **44**, 2300020.
- 63 B. G. G. Lohmeijer, G. Dubois, F. Leibfarth, R. C. Pratt, F. Nederberg, A. Nelson, R. M. Waymouth, C. Wade and J. L. Hedrick, Organocatalytic Living Ring-Opening Polymerization of Cyclic Carbosiloxanes, *Org. Lett.*, 2006, **8**, 4683–4686.
- 64 V. Nair, S. Bindu and V. Sreekumar, N-Heterocyclic Carbenes: Reagents, Not Just Ligands, *Angew. Chem., Int. Ed.*, 2004, **43**, 5130–5135.
- 65 S. Naumann and M. R. Buchmeiser, Liberation of N-heterocyclic carbenes (NHCs) from thermally labile progenitors: protected NHCs as versatile tools in organo- and polymerization catalysis, *Catal. Sci. Technol.*, 2014, **4**, 2466–2479.
- 66 C. De Risi, A. Brandolese, G. Di Carmine, D. Ragno, A. Massi and O. Bortolini, Oxidative N-Heterocyclic Carbene Catalysis, *Chem.–Eur. J.*, 2023, **29**, e202202467.



- 67 L. He, H. Guo, Y. Wang, G.-F. Du and B. Dai, N-heterocyclic carbene-mediated transformations of silicon reagents, *Tetrahedron Lett.*, 2015, **56**, 972–980.
- 68 A. P. Dove, R. C. Pratt, B. G. G. Lohmeijer, D. A. Culkin, E. C. Hagberg, G. W. Nyce, R. M. Waymouth and J. L. Hedrick, N-Heterocyclic carbenes: effective organic catalysts for living polymerization, *Polymer*, 2006, **47**, 4018–4025.
- 69 S. Csihony, D. A. Culkin, A. C. Sentman, A. P. Dove, R. M. Waymouth and J. L. Hedrick, Single-Component Catalyst/Initiators for the Organocatalytic Ring-Opening Polymerization of Lactide, *J. Am. Chem. Soc.*, 2005, **127**, 9079–9084.
- 70 A. Hoppe, F. Sadaka, C.-H. Brachais, G. Boni, J.-P. Couvercelle and L. Plasseraud, 1-n-Butyl-3-methylimidazolium-2-carboxylate: a versatile precatalyst for the ring-opening polymerization of  $\epsilon$ -caprolactone and lactide under solvent-free conditions, *Beilstein J. Org. Chem.*, 2013, **9**, 647–654.
- 71 D. C. M. Albanese and N. Gaggero, An Overview on the N-Heterocyclic Carbene-Catalyzed Aza-Benzoin Condensation Reaction, *Catalysts*, 2018, **8**, 181.
- 72 M. Fèvre, P. Coupillaud, K. Miqueu, J.-M. Sotiropoulos, J. Vignolle and D. Taton, Imidazolium Hydrogen Carbonates versus Imidazolium Carboxylates as Organic Precatalysts for N-Heterocyclic Carbene Catalyzed Reactions, *J. Org. Chem.*, 2012, **77**, 10135–10144.
- 73 M. Fèvre, J. Pinaud, Y. Gnanou, J. Vignolle and D. Taton, N-Heterocyclic carbenes (NHCs) as organocatalysts and structural components in metal-free polymer synthesis, *Chem. Soc. Rev.*, 2013, **42**, 2142–2172.
- 74 N. Konstandaras, M. H. Dunn, E. T. Luis, M. L. Cole and J. B. Harper, The  $pK_a$  values of N-aryl imidazolium salts, their higher homologues, and formamidinium salts in dimethyl sulfoxide, *Org. Biomol. Chem.*, 2020, **18**, 1910–1917.
- 75 M. H. Dunn, N. Konstandaras, M. L. Cole and J. B. Harper, Targeted and Systematic Approach to the Study of  $pK_a$  Values of Imidazolium Salts in Dimethyl Sulfoxide, *J. Org. Chem.*, 2017, **82**, 7324–7331.
- 76 F. Van Lijsebetten, S. Maes, J. M. Winne and F. E. Du Prez, Thermoswitchable catalysis to inhibit and promote plastic flow in vitrimers, *Chem. Sci.*, 2024, **15**, 7061–7071.
- 77 B. P. Maliszewski, E. Casillo, P. Lambert, F. Nahra, C. S. J. Cazin and S. P. Nolan, Simply accessible platinum(ii) complexes enabling alkene hydrosilylation at ppm catalyst loadings, *Chem. Commun.*, 2023, **59**, 14017–14020.
- 78 B. P. Maliszewski, T. A. C. A. Bayrakdar, P. Lambert, L. Hamdouna, X. Trivelli, L. Cavallo, A. Poater, M. Beliš, O. Lafon, K. Van Hecke, D. Ormerod, C. S. J. Cazin, F. Nahra and S. P. Nolan, PtII-N-Heterocyclic Carbene Complexes in Solvent-Free Alkene Hydrosilylation, *Chem.–Eur. J.*, 2023, **29**, e202301259.
- 79 D. Troegel and J. Stohrer, Recent advances and actual challenges in late transition metal catalyzed hydrosilylation of olefins from an industrial point of view, *Coord. Chem. Rev.*, 2011, **255**, 1440–1459.
- 80 O. Hollóczki, The Mechanism of N-Heterocyclic Carbene Organocatalysis through a Magnifying Glass, *Chem.–Eur. J.*, 2020, **26**, 4885–4894.
- 81 S. Tshepelevitsh, A. Kütt, M. Lökov, I. Kaljurand, J. Saame, A. Heering, P. G. Plieger, R. Vianello and I. Leito, On the Basicity of Organic Bases in Different Media, *Eur. J. Org. Chem.*, 2019, **2019**, 6735–6748.
- 82 A. P. Bento and F. M. Bickelhaupt, Nucleophilic Substitution at Silicon (SN2@Si) via a Central Reaction Barrier, *J. Org. Chem.*, 2007, **72**, 2201–2207.
- 83 D. Rico del Cerro, R. Mera-Adasme, A. W. T. King, J. E. Perea-Buceta, S. Heikkinen, T. Hase, D. Sundholm and K. Wähälä, On the Mechanism of the Reactivity of 1,3-Dialkylimidazolium Salts under Basic to Acidic Conditions: A Combined Kinetic and Computational Study, *Angew. Chem., Int. Ed.*, 2018, **57**, 11613–11617.
- 84 S. Gehrke and O. Hollóczki, N-Heterocyclic Carbene Organocatalysis: With or Without Carbenes?, *Chem.–Eur. J.*, 2020, **26**, 10140–10151.
- 85 N. V. Tzouras, F. Nahra, L. Falivene, L. Cavallo, M. Saab, K. Van Hecke, A. Collado, C. J. Collett, A. D. Smith, C. S. J. Cazin and S. P. Nolan, A Mechanistically and Operationally Simple Route to Metal–N-Heterocyclic Carbene (NHC) Complexes, *Chem.–Eur. J.*, 2020, **26**, 4515–4519.
- 86 M. F. Silva Valverde, E. Theuergarten, T. Bannenberg, M. Freytag, P. G. Jones and M. Tamm, Frustrated N-heterocyclic carbene–silylium ion Lewis pairs, *Dalton Trans.*, 2015, **44**, 9400–9408.
- 87 F. Van Lijsebetten, Y. Spiesschaert, J. M. Winne and F. E. Du Prez, Reprocessing of Covalent Adaptable Polyamide Networks through Internal Catalysis and Ring-Size Effects, *J. Am. Chem. Soc.*, 2021, **143**, 15834–15844.
- 88 C. Xu and Z. Cheng, Thermal Stability of Ionic Liquids: Current Status and Prospects for Future Development, *Processes*, 2021, **9**, 337.
- 89 H. Münstedt, Rheological experiments at constant stress as efficient method to characterize polymeric materials, *J. Rheol.*, 2014, **58**, 565–587.
- 90 R. G. Ricarte and S. Shanbhag, Unentangled Vitriimer Melts: Interplay between Chain Relaxation and Cross-link Exchange Controls Linear Rheology, *Macromolecules*, 2021, **54**, 3304–3320.

